Available online at www.sciencedirect.com
ScienceDirect
Polymer 48 (2007) 4567–4577
polymer
www.elsevier.com/locate/polymer

Kinetic analysis on spherulite growth rate of polypropylene catalloys

Yonggang Shangguan [a,b], Yihu Song [a,b], Qiang Zheng [a,b,*]

[a] Department of Polymer Science and Engineering, Zhejiang University, Hangzhou 310027, PR China
[b] Key Laboratory of Macromolecular Synthesis and Functionalization, Ministry of Education, Hangzhou 310027, PR China

Received 8 December 2006; received in revised form 19 April 2007; accepted 18 May 2007
Available online 2 June 2007

Abstract

The kinetic analysis on melt-crystallization of polypropylene catalloys (PP-cats) was conducted through measuring their spherulite growth rates. A multiple melting behavior of PP-cats was found through differential scanning calorimetry (DSC) and the corresponding crystalline microstructures of PP-cats were studied by wide-angle X-ray diffraction (WAXD). The calculated T_m^o value of propylene homopolymer (PP) suggests an obvious melting point depression of PP-cats. Moreover, it is found that the existence of ethylene–propylene copolymer could result in the changes of crystalline microstructure of PP and the PP crystal is in favor of growing along (040) lattice plane of α-monoclinic crystal. The crystal growth rate of PP-cats decreases with the increase of ethylene–propylene copolymer content in PP-cats. A comparison of crystallization kinetics between PP-cats and virgin iPP through a modified Lauritzen–Hoffman model indicates that there appears a transition from regimes II to III in iPP and PP-cats containing low ethylene–propylene copolymer content. However, for the PP-cats containing high ethylene–propylene copolymer content, crystallization always processes in regime II. In addition, both calculated nucleation parameter (K_g) and the fold surface free energy (σ_e) for PP-cats increase with the increase of ethylene–propylene copolymer content, implying that the existence of ethylene–propylene copolymer is unfavorable for the surface nucleation of PP and regular folding of the molecule chain. It is believed that an increase in viscosity of the melts induced by different compositions could remarkably slow crystallization growth down, because under this condition surface nucleation dominates as compared with crystal growth.

Keywords: Polypropylene catalloys; Spherulite growth rate; Crystallization kinetics

1. Introduction

As an *in situ* polypropylene alloy, Polypropylene catalloys (PP-cats) consist mainly of three compositions: propylene homopolymer (PP), ethylene–propylene random copolymer (EPR) and ethylene–propylene block copolymer [1,2]. In comparison with general polypropylenes modified by mechanical blending with thermoplastic elastomer, PP-cats can provide better mechanical properties and production costs. Like most of polymer blends, performances of PP-cats depend strongly on microstructure and morphology formed during processing. Because PP is a main component in PP-cats, its crystallization behavior plays an important role in its structure and morphology. In view of the importance in industrial aspects and academic research, it is necessary for us to investigate the crystallization behavior and kinetics of PP-cats experimentally and theoretically.

It has widely been accepted that the crystallization of polymers from the melted state could be divided into three stages: primary nucleation, crystal growth and secondary crystallization. Primary nucleation is the process in which a crystalline nucleus forms in the melt state homogeneously or heterogeneously. Consequently, crystalline lamellas develop and three-dimensional superstructures form. The most common morphology encountering solidification from the melt is the spherulite; however, other superstructures, such as hedrites or dendrites, form as well [3]. Since the isothermal experiment is considerably easy to control, the traditional method of measuring crystal growth rate of polymeric materials is conducted in this condition.

* Corresponding author. Department of Polymer Science and Engineering, Zhejiang University, Hangzhou 310027, PR China. Tel./fax: +86 571 8795 2522.
E-mail address: zhengqiang@zju.edu.cn (Q. Zheng).

0032-3861/$ - see front matter © 2007 Elsevier Ltd. All rights reserved.
doi:10.1016/j.polymer.2007.05.066

However, it should consume too many time for one to probe crystal growth rates in an entire temperature range, because only a growth rate at the isothermal condition could be achieved through an experiment at a given temperature. Furthermore, with the decrease of temperature, the high degree of supercooling for the melt usually makes the crystallization rate too fast and nucleation density too high at lower temperatures, and consequently, leads to a difficulty in measuring crystal growth rate at lower temperatures.

Chen and Chung [4] proposed an alternative technique to conventional time-consuming isothermal methods. According to their results dealing with poly(ether ether ketone) (PEEK) obtained by using one single measurement, it is possible to obtain isothermal solidification data that would require several separate experiments with isothermal methods. Di Lorenzo et al. [5] developed this procedure by using different cooling rates and investigated the crystal growth rates of iPP/poly-(a-pinene) blends. It is found that the temperature region measured is very narrow in the case of isothermal measurement and could be expanded using different cooling rates, especially under low temperatures at which isothermal experimental observation could hardly be conducted. We have reported some characteristics of PP-cats crystallization such as crystalline structure, morphology, and crystallization rate [6,7] and found the annealing treatment for PP-cats at 200 °C could hardly result in the changes of both crystallization and melting behavior for PP-cats [8]. In the present article, we attempt to probe the crystal growth rates of PP-cats through isothermal and nonisothermal methods, and discuss the effects of composition of PP-cats on crystallization kinetics based on a modified Lauritzen–Hoffman model [9–11].

2. Experimental

2.1. Materials and sample preparation

The grade of polypropylene (T300, isotactic homopolymer, $\overline{M}_n = 80\,643$ and $\overline{M}_w = 333\,465$, isotacticity = 96%) used here was supplied by Sinopec Shanghai Petrochemical Co. of China.

PP-cats were supplied by the Institute of Polymer Science of Zhejiang University, China. The synthesis of PP-cats includes three steps, *i.e.*, pre-polymerization of propylene, bulk polymerization of propylene, and gas-phase copolymerization of ethylene and propylene. The synthesis details have been described in previous paper [2]. The PP-cats were designated as PEP20, PEP30, PEP40, PEP50 and PEP60, respectively, in which capital E stands for ethylene component and the numerals represent its percentage used in the gas-phase copolymerization in the third stage, respectively. The content of ethylene and ethylene–propylene copolymer in the catalloys and the melting flow indices (MFI) of these specimens are listed in Table 1.

The iPP and PP-cats samples were prepared by compression-molding at 200 °C with a pressure of 10 MPa for 5 min, then the pressure was released and the molded samples were removed from the press and cooled down to room temperature.

Table 1
The characteristic parameters of iPP and PP-cats

Samples	Content of ethylene (mol%)	Content of ethylene–propylene copolymer (wt%)	MFI[a] (g/10 min)
iPP	–	–	3.00
PEP20	2.87	17.8	1.54
PEP30	3.10	19.9	1.38
PEP40	11.80	23.2	1.27
PEP50	17.80	30.0	–
PEP60	27.10	34.2	0.56

[a] Measured at 230 °C and 21.2 N load.

The film samples with thickness of 60 μm were used to FT-IR, DSC and POM measurements.

2.2. Composition identification of PP-cats

To separate the random copolymer from PP-cats, a modified Kumagawa extractor was used to conduct a temperature-gradient extraction fractionation of PP-cats [12]. Firstly, about 10 g of PP-cats sample was dissolved at 50 °C in *n*-octane and stirred violently for 2 h. To avoid the oxidation of EPR, the sample was doped with 0.1 wt% of the antioxidant. The filtrate was obtained and was then precipitated and washed by acetone, dried in vacuum. The weight percentage of the fraction was used to evaluate the content of random copolymer in the blends [1]. Secondly, the insoluble remaining samples were extracted at 105 °C in a Kumagawa extractor by boiling *n*-octane for 24 h, and the extracted solution was concentrated and precipitated by ethanol, then washed and consequently dried in vacuum. The weight percentage of the fraction was used as a criterion of the content of block copolymer in the blends. The insoluble parts were washed with *n*-octane and dried in vacuum. The weight percentage of soluble parts was applied to the analysis of the propylene homopolymer in the blend. Here, propylene homopolymers separated from various PP-cats are referred as PP20, PP30, PP40, PP50 and PP60, respectively. Fig. 1 gives the component data of PP-cats.

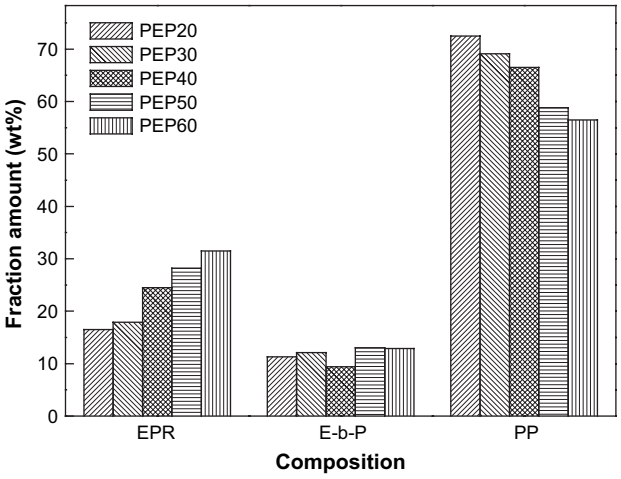

Fig. 1. The fractions distribution of PP-cats samples.

Table 2
The characteristics parameters for propylene homopolymer fractions in PP-cats

Samples	$\overline{M}_w$ [a]	$\overline{M}_w/\overline{M}_n$ [a]	Isotacticity (%)[b]
PP20	79 354	2.31	96.0
PP30	80 938	2.21	95.7
PP40	83 546	1.83	95.8
PP50	91 372	1.71	95.4
PP60	93 251	1.64	96.0

[a] Determined by GPC.
[b] Calculated from FT-IR data.

2.3. Gel permeation chromatography (GPC)

Weight-average molecular weight ($\overline{M}_w$) and polydispersity of molar mass for fractionated propylene homopolymers were determined by gel permeation chromatography (GPC) at 150 °C. The GPC system used is a PL-GPC220 equipped with three PLgel 10 mm MIXED-B columns using polystyrene as standard and 1,2,4-trichlorobenzene (1.0 mL min^{-1}) as the eluent. Table 2 lists the molecular weight and polydispersity data of propylene homopolymer extracted from PP-cats.

2.4. Fourier-transfer infrared spectra (FT-IR)

The Fourier-transfer infrared spectra of the thin hot-pressing sample films for fractionated propylene homopolymers were recorded on a Nicolet 5DX FT-IR spectrometer. The isotacticity of fractionated PP was also calculated from FT-IR data using the following equation

$$\mathrm{IIP} = K \times A_{975}/A_{1460} \tag{1}$$

in which K is a constant relevant to apparatus. A_{975} and A_{1460} are the absorbtion peak areas for isotactic helical segment and methyl, respectively. Table 2 lists the calculated isotacticity data of propylene homopolymer extracted from PP-cats.

2.5. Differential scanning calorimetry (DSC)

A Perkin–Elmer series 7 differential scanning calorimeter (DSC) with N_2 as purge gas was used to investigate the isothermal crystallization behavior of the iPP and PP-cats. Pure indium and zincum were used as reference materials to calibrate both the temperature scale and the melting enthalpy before the samples were tested. The samples (~5.0 mg) were heat-treated at 200 °C for 10 min to eliminate the thermal history, and then quenched down to the crystallization temperature (T_c) to complete the isothermal crystallization. Subsequently, the melting traces were recorded at a heating rate of 10 °C/min. The percentage of β-iPP crystals for PP-cats, ϕ_β, was determined by the relative crystallinity of α- and β-iPP calculated from DSC data, as described in Ref. [6].

2.6. Wide angle X-ray diffraction (WAXD)

Wide-angle X-ray diffraction (WAXD) patterns were obtained using a Rigaku D/max-IIIB diffractometer with the Cu Kα radiation at room temperature. The condition tested was set at a voltage of 40 kV and a current of 300 mA in a range of $2\theta = 0–40°$ at room temperature. The samples of iPP and PP-cats which completed isothermal crystallization during POM measurement were used for WAXD measurements.

2.7. Optical microscope (OM)

A real-time observation for crystallization process and spherulite growth was performed by using a CCD color camera linked with polarized optical microscope (POM) in constant interval. The samples were sandwiched between two microscope cover slips for observation. The crystal growth rates were measured using isothermal and nonisothermal methods, respectively. The isothermal experiments were conducted in the temperature range from 130 to 154 °C. The sample was first heated to 200 °C for 10 min in order to erase the thermomechanical history, and then moved to a preheated hot stage where the sample crystallized at given temperature T_c. Timing of the crystallization process started as soon as the sample was placed on the hot stage, and the morphologies were recorded at constant time intervals. The spherulite radius (r) was measured through a comparison between the recorded micrographs and the standard micrograph of tacheometer staff. The growth rate (G) of polymer spherulites was obtained from the slope of the plot of r vs. time (t) at the given T_c.

$$G = \frac{\mathrm{d}r}{\mathrm{d}t} \tag{2}$$

The crystal growth rates were also calculated under nonisothermal condition. The samples were preheated at 200 °C for 10 min, and then cooled to room temperature at different cooling rates from 0.5 to 5 °C/min. The diameters of a series of spherulites grown for different time periods were measured and G value was calculated by using the equation proposed by Chen and Chung [4]

$$\frac{\mathrm{d}r}{\mathrm{d}t} = \frac{\mathrm{d}r}{\mathrm{d}T} \cdot \frac{\mathrm{d}T}{\mathrm{d}t} \tag{3}$$

where $\mathrm{d}r/\mathrm{d}t$, $\mathrm{d}T/\mathrm{d}t$ and $\mathrm{d}r/\mathrm{d}T$ are the radial growth rate, the cooling rate and the first derivative of the plot of r vs. T at each experimental point, respectively.

Adopted data for spherulite growth rate were averages of at least five measurements. The precision of controlled hot-stage is less than ±1.0 °C. All images presented in this work were taken under the crossed-polarized condition. Dry N_2 was purged through the hot stage in all heating and cooling processes.

3. Results and discussion

3.1. Melting behavior and equilibrium melting temperature of PP-cats

Fig. 1 gives the fractions distribution of various PP-cats samples. It can be found that the content of propylene homopolymer is highest among three components for all PP-cats. The melting behavior and crystalline structure of PP-cats

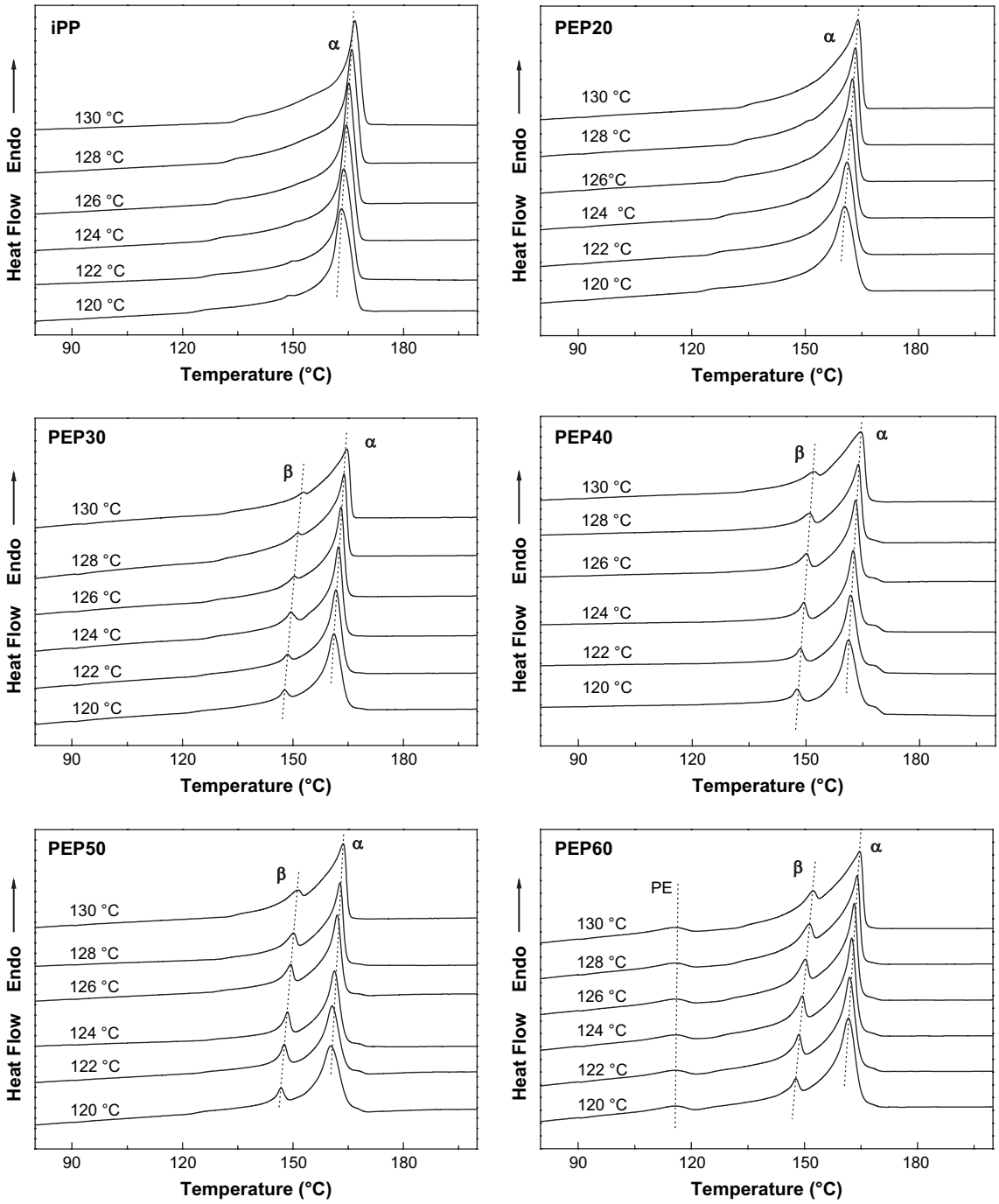

Fig. 2. DSC melting traces of iPP and various PP-cats samples isothermally crystallized at different temperatures.

samples subjected to nonisothermal crystallization have been described and the multiple melting behavior of PP-cats, depending on the composition and cooling condition, has been observed in our previous paper [6,7]. Fig. 2 gives the melting traces of iPP and various PP-cats samples isothermally crystallized at different temperatures. It is obvious that iPP sample only presents single melting peak at about 165 °C and the peak temperature shifts toward high temperature with the increase of crystallization temperature. These results show that only α-crystal of iPP forms during isothermal crystallization under investigation and the crystalline perfection of iPP improves with increase of crystallization temperature. Similar to pure iPP, PEP20 samples also demonstrate only single peak resulting from the melting of α-iPP. However, for other PP-cats, at least two melting peaks can be observed. For PEP30, PEP40 and PEP50 samples crystallized at different temperatures, a small melting peak at about 150 °C appears besides the melting peak of α-iPP at 165 °C. The WAXD and the POM observations show that the small melting peak results from the melting of β-iPP. Furthermore, an obvious melting peak is observed at about 118 °C for PEP60 samples and its peak temperature is unchangeable with the increase of

Table 3
β-iPP content of PP-cats samples crystallized at different isothermal conditions

Crystallization temperature (°C)	PEP20 (%)	PEP30 (%)	PEP40 (%)	PEP50 (%)	PEP60 (%)
120	–	1.13	1.87	2.35	2.46
122	–	1.24	2.02	3.68	4.71
124	–	1.76	2.89	3.91	6.18
126	–	1.39	0.71	2.75	2.50
128	–	0.95	0.54	2.56	2.21
130	–	0.58	0.36	1.26	1.91

Calculated from DSC data.

crystallization temperature. Depending on WAXD tests, the melting peak is ascribed to the melting of polyethylene crystal. Table 3 lists the β-iPP content in crystalline phase of various PP-cats crystallized at different temperatures. It can be seen that the content of β-iPP is dependent on the crystallization temperature, and 124 °C is the most favorable temperature to obtain β-iPP for PP-cats. It is reasonable to ignore the existence of β-iPP considering the melting behavior of PP-cats because of the few content of β-iPP.

The equilibrium melting temperature of semi-crystalline polymer T_m^o denotes the melting temperature of the infinite crystal with extended chain conformation and the greatest degree of perfection. One of the most commonly used procedures to determine T_m^o is the Hoffman–Weeks equation [13] as given as

$$T_m = T_m^o(1 - 1/\gamma) + T_c/\gamma \quad (4)$$

where T_m is the observed melting temperature, T_c is the crystallization temperature, and $\gamma = l/l^*$ is the ratio of the lamellar thickness l to the thickness l^* of the critical nuclei at T_c, respectively. The T_m^o value could be easily obtained from the classic Hoffman–Weeks plot. Fig. 3 gives the dependence of melting peak temperature of iPP and PP-cats on crystallization temperatures. It can be seen that the peak temperatures of PP-cats increase with the increase of crystallization

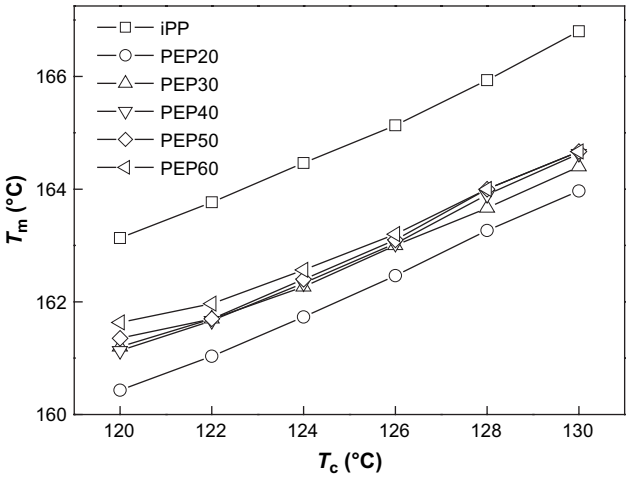

Fig. 3. Melting temperatures of iPP and PP-cats crystallized at different temperatures.

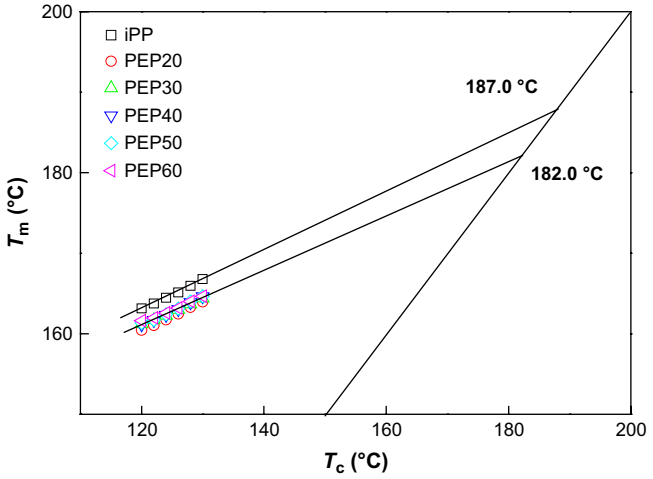

Fig. 4. Hoffman–Weeks plots of iPP and PP-cats.

temperature, indicating improvement of the crystalline perfection for PP-cats with the increase of crystallization temperature. Fig. 4 gives the Hoffman–Weeks plots of iPP and PP-cats. The T_m^o values of 187 °C for iPP and 182 °C for PP-cats could be obtained by extrapolating the experimental data to $T_m = T_c$ line. For iPP, the T_m^o value coincides well with that reported [14]. It is interesting that the T_m^o of PP-cats seems independent of the compositions, but an obvious melting point depression can be observed. Table 2 lists the molecular weight, polydispersity and the isotacticity of PP component separated from PP-cats. The weight-average molecular weight of PP slightly increases from PP20 to PP60 and its polydispersity narrows, but their isotacticity data is basically equivalent. Compared with pure iPP, propylene homopolymers in PP-cats have lower molecular weight and narrower polydispersity. However, the isotacticity of propylene homopolymer in PP-cats is the same as that of iPP. On the other hand, the interaction between PP and EPR components in PP-cats is stronger than that of general iPP/EPR blends because of the existence of ethylene–propylene block copolymer [6,15,16]. Thus, it suggests that melting point depression of PP-cats lies in two factors: one is the lower molecular weight of propylene homopolymer, and the other is the stronger interactions between compositions in PP-cats.

3.2. Crystalline structure

Fig. 5 gives the WAXD patterns of iPP and PP-cats crystallized isothermally at 124 °C. It can be found that for iPP and PEP20, the existences of diffraction peaks at 2θ angles of 14.0, 16.8, 18.6, 21.2 and 21.9°, corresponding to the (110), (040), (130), (111) and $(13.\bar{1})$ lattice planes, indicate that crystalline phase mainly consists of α-monoclinic crystal. However, for other PP-cats, a small diffraction peak at 16.0° could also be observed, besides the diagnostic diffraction peaks of α-iPP. These results suggest the existence of β-iPP crystal in crystallized PP-cats sample and can be used to explain their multiple melting behavior. In diffraction intensity theory, the diffraction intensity which prefers the peak area instead of peak height,

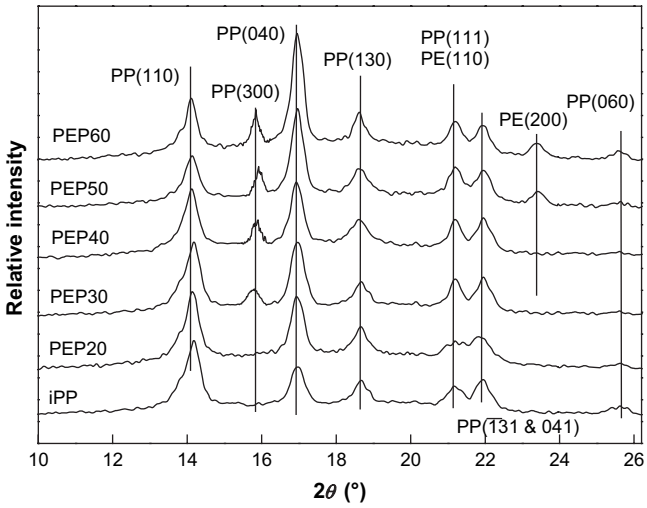

Fig. 5. WAXD patterns of iPP and PP-cats crystallized isothermally at 124 °C.

depends on the size and number of the microcrystal in three axes, and for α-iPP crystal the normal line direction for (040) lattice plane is in agreement of *b* axis [17]. For most bulk crystallization cases of iPP, the diffraction peak of (110) lattice plane corresponding to $2\theta = 14.0^{\circ}$ presents the highest diffraction intensity, in accord with the iPP WAXD pattern in Fig. 5. However, the diffraction intensity of (110) lattice plane for all PP-cats is less than that of (040) lattice plane, meaning that along (040) lattice plane is the most preferential direction for crystal growth in PP-cats, and by contraries, the growth along (110) lattice plane direction is restricted to some extent. It can also be found that the half-peak width of (040) diffraction peak of these samples decreases from PEP20 to PEP60, indicating that the crystal size generally increases. These results are in accordance with the crystallization behavior of ethylene–propylene copolymers [18]. It is noted that for melt crystallization of block polymer or polymer blends, the space growth of crystallizable segments is dependent on the interactions of adjacent groups and segments [18]. Hence, the highest diffraction intensity of (040) lattice plane of PP-cats implies that, for crystallizable segments, the force along *b* axis is minimal during crystal growth of PP-cats. Furthermore, it can be seen from WAXD patterns of PP-cats that there appears regular change with the composition of PP-cats in the relative diffraction intensity of (040) lattice plane. These results reveal that the different crystalline structures of PP-cats mainly depend on the composition instead of crystallization conditions.

3.3. Spherulite growth rates

For iPP/EPR blends, although all of them have been proved to be immiscible at molten state and most of them are also immiscible below the crystallization temperature of iPP, some miscible blends with special composition can be obtained through some methods at room temperature [19]. We have reported the effects of annealing temperature and time at melt state on the crystallization and melt behavior of PP-cats and found that the different annealing time at 200 °C have little effect on crystallization and melt behavior of PP-cats, but the annealing treatment at 220 °C could result in the remarkable changes of crystallization and melt behavior for PP-cats [8].

The optical microscopic observation demonstrates that for all PP-cats under investigation, no obvious segregated domains in the melt can be observed for different annealing time from 10 to 60 min at 200 °C by using optical microscope. These imply that the domain dimension of the dispersed phases is below the resolution of optical microscopy, and at 200 °C no obvious liquid–liquid phase separation happens in the time range observed. Under isothermal crystallization, the morphology changes remarkably with the evolvement of the time, since a liquid–solid phase separation resulting from the iPP crystallization takes place at T_c. It should be pointed out that the remaining amorphous phase is visibly homogeneous under optical microscope after new phases (iPP crystalline phase) form through crystallization. Fig. 6 gives the morphology of iPP and PP-cats crystallized isothermally at 140 °C for 80 min (timing starts when the first clear nuclei can be distinguished). The clear spherulite profiles can be observed for all PP-cats, and the differences of both spherulite size and nucleation density are very obvious among iPP and PP-cats. In addition, above morphological characteristic can be found at all temperatures. These results indicate that the melt-crystallization of PP-cats proceeds with spherulite growth mode. It is noted that the microphase separation state of PP-cats samples has been found by DMA data [20], although the microdomains could hardly be observed by optical microscopy because of limited resolution. Thus, the primary nucleation rate of PP increasing with the increase in the ethylene content may be ascribed to the nucleation effect of EPR microdomain on PP.

It is well accepted that the crystal growth rates of homopolymers are constant at a given temperature. However, for polymer blends, they may be variable, involving in the interactions between components [21,22]. Fig. 7 gives the dependence of spherulite radius on crystallization time for several PP-cats samples crystallized isothermally at 140 °C. For every spherulite observed, the timing starts when the clear nuclei profile can be distinguished. The reported spherulite radius data is an average value of at least five spherulites. All the spherulite growths of PP-cats appear linear time-dependence, similar to that of homopolymers. Moreover, the slope of the curve generally decreases with the increase of ethylene content in PP-cats, which indicates that the crystal growth rate depends on PP-cats composition.

Fig. 8 presents the spherulite growth rates of PP-cats samples which were exposed to annealing treatment for different time intervals at 200 °C before crystallization. It can be seen that for PEP20 and PEP60 samples, the values of spherulite growth rate present little difference at the given temperature. For other PP-cats, similar experimental results can be observed. These results are in accord with the above morphology results, indicating that no obvious liquid–liquid phase separation happens in the melt state of PP-cats and the effect of liquid–liquid phase separation is reasonable to be ignored for evaluating crystal growth rate of PP-cats.

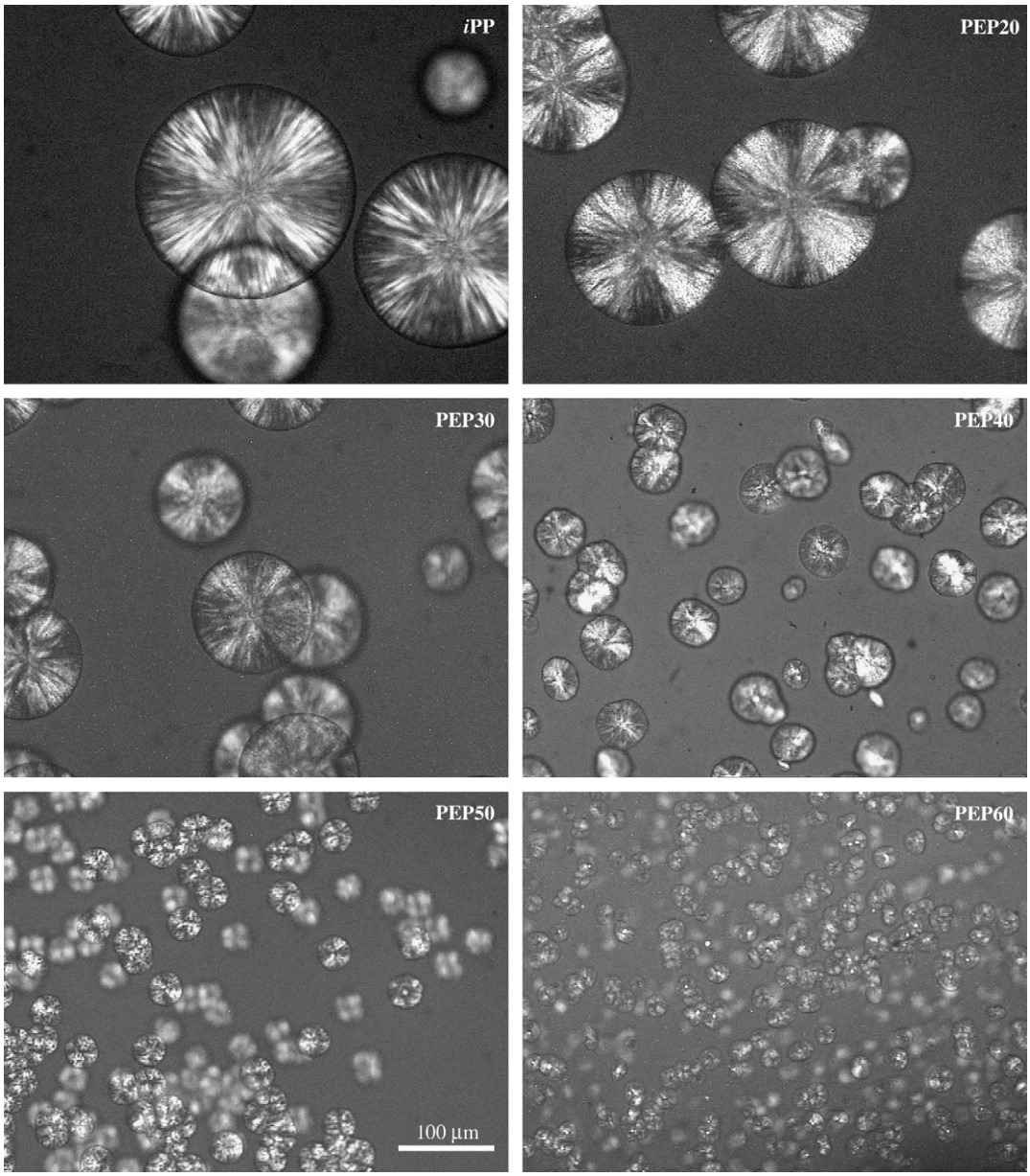

Fig. 6. Optical microscope images for iPP and PP-c crystallized isothermally at 140 °C for 80 min.

Fig. 9(a) gives the spherulite growth rate obtained through isothermal method at different temperatures for pure iPP and various PP-cats. Even though spherulite growth rates of all PP-cats are smaller than that of pure iPP, the spherulite growth rates of PP-cats present distinct component-dependence and they decrease with the increase of ethylene–propylene copolymer content in PP-cats. In general, for melt crystallization, higher temperatures can result in the decrease of the degree of supercooling and consequently the decrease of crystal growth rate. Accordingly, the differences in spherulite growth rates between PP-cats and pure iPP samples appear obvious, especially at lower temperatures, and become very small with the increase of crystallization temperature. Moreover, it can be found from the enlarged figure that at high temperatures (140–155 °C), PP-cats still present obvious component-dependent spherulite growth rate. Considering the increase of viscosities of PP-cats with the increase of ethylene content, we believe that the high viscosity probably results in a decrease in the motion ability of the crystallizable propylene segments and consequently a decrease in spherulite growth rate.

It has been reported in our previous paper that it is valid to obtain the spherulite growth rates of PP-cats using nonisothermal method [6]. Fig. 9(b) gives the calculated spherulite growth rates of PP-cats and pure iPP through nonisothermal method. These data present similar temperature-dependence. Here, the temperature suitable for measuring through nonisothermal method is lower than that through isothermal method. Moreover, it could be found that the lowest temperatures at which the spherulite growth rate could be measured are different for various PP-cats samples, and seem to be involved in the composition.

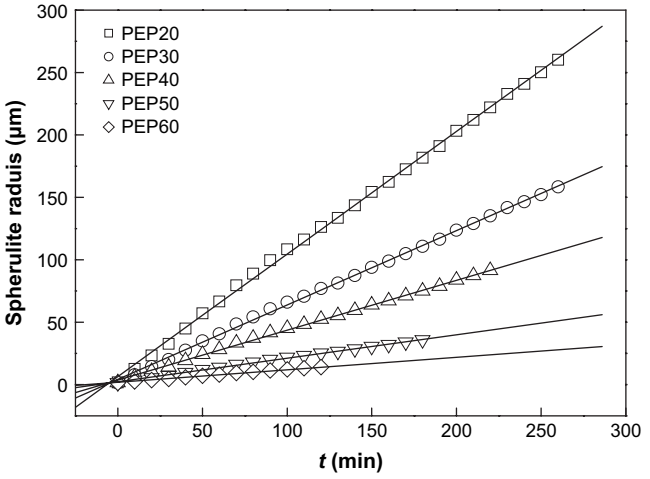

Fig. 7. Dependence of spherulite radius of PP-cats samples on crystallization time at $T_c = 140\ ^\circ C$.

3.4. Crystallization kinetics

Lauritzen–Hoffman model [23] has been widely applied to examine the crystallization kinetics of polymeric materials, especially for those at melt-crystallization condition.

$$G = G_0 \exp\left[\frac{-U^*}{R(T_c - T_\infty)}\right] \exp\left[\frac{-K_g}{T_c \cdot \Delta T \cdot f}\right] \quad (5)$$

where G_0 is a preexponential term, U^* is the energy for the transport of the macromolecules in the melt, R is the universal gas constant, T_c is the crystallization temperature, T_∞ is the temperature at which all the motions associated with the viscous flow stop and is defined as $T_\infty = T_g - C$, here C is a constant that can assume different values, in this paper $C \approx 30$ K. ΔT is the undercooling ($\Delta T = T_m^o - T_c$), here T_m^o is the equilibrium melting temperature. f is a corrective factor responsible for the variation of the equilibrium melting enthalpy with

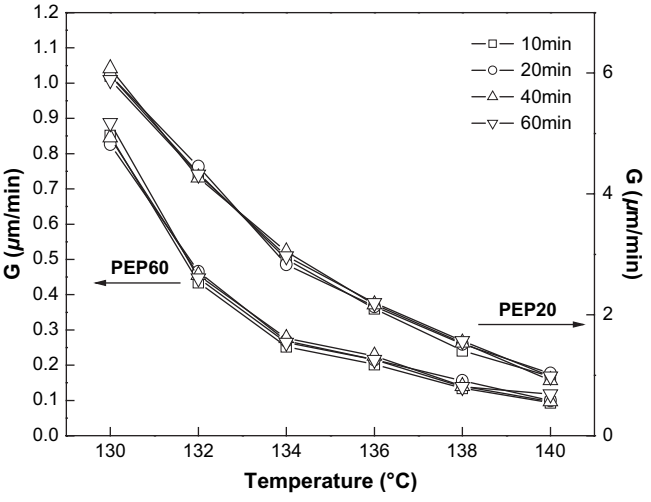

Fig. 8. Spherulite growth rates of PEP20 and PEP60 crystallized at different temperatures after the samples were annealed at 200 °C for different time intervals.

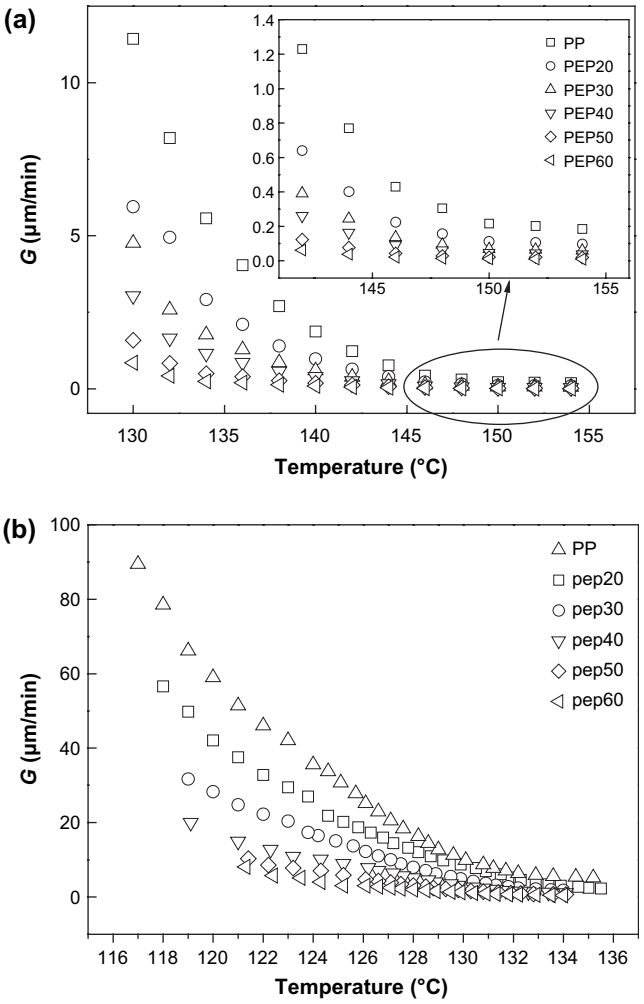

Fig. 9. Spherulite growth rates measured at isothermal conditions (a) and nonisothermal conditions (b) for iPP and PP-cats crystallized at different temperatures.

temperature, defined as $f = 2T_c/(T_m^o + T_c)$, and K_g is nucleation parameter dealing with the energy required for the formation of nuclei of critical size as defined as

$$K_g = nb_0\sigma_e T_m^o / \Delta h_f k \quad (6)$$

where n is a variable depending on the crystallization regime, b_0 is the layer thickness, σ is the lateral surface free energy, σ_e is the fold surface free energy, k is the Boltzmann constant, and Δh_f is the enthalpy of fusion.

Eq. (5) can be re-written as

$$\ln G = \ln G_0 - \left[\frac{U^*}{R(T_c - T_\infty)}\right] - \left[\frac{K_g}{T_c \cdot \Delta T \cdot f}\right] \quad (7)$$

Regime transitions are observed experimentally as abrupt changes of slope in plots of $\ln G + U^*/R(T_c - T_\infty)$ against $1/(f \cdot T_c \cdot \Delta T)$. Growth of crystals can occur in different regimes, depending on temperature. At high temperatures (low undercooling), formation of a surface secondary nucleus is followed by rapid completion of the substrate, which is referred to as regime I, and n equals to 4. At lower temperatures, in

Table 4
Values of iPP materials constants

α-iPP	3_1 Helix	110 Growth plane	
T_m^o	187 °C	a_o	5.49 Å
T_g	−12 °C	b_o	6.26 Å
Δh_f	178 × 0.936 J/cm^3	$a_o b_o$	34.37 Å
Unit cell parameters		040 Growth plane	
a	6.65 Å	a_o	6.56 Å
b	20.96 Å	b_o	5.24 Å
c	6.50 Å	$a_o b_o$	34.37 Å
β	99.3°		

regime II, multiple surface nuclei form on the substrate and spread out slowly, and n equals 2. At even lower temperatures, when solidification takes place in regime III, a large number of surface nuclei form so that the distance between two nuclei approximates the width of a stem and n equals 4. From Eq. (6), the K_g relation between different regimes equation can be hold: $K_g(\mathrm{I}) = K_g(\mathrm{III}) = 2K_g(\mathrm{II})$. The general understanding lies in that in regime III which occurs at temperatures lower than regimes I and II, the mobility of polymer chains is low.

Being an important kinetic parameter, the fold surface free energy couldn't be directly obtained. However, the lateral surface free energy, α, can be calculated by

$$\alpha = a\Delta h_f (a_o b_o)^{1/2} \tag{8}$$

where the value of $\alpha = 0.1$ was assumed to be universal and $a_o b_o$ is the cross-sectional area of the chain [24]. In general, the crystal phase of iPP is mainly α-crystal and the crystal growth is in favor along (110) lattice plane during melt-crystallization. However, on the basis of above analysis on crystalline phase structure, it is understood that the crystal growth of PP-cats is in favor along (040) lattice plane. Table 4 lists the unit cell parameters of iPP [24]. It can be found that the values of $a_o b_o$ are the same for two different crystal growth surfaces, indicating the calculated σ value is independent of the growth mode. The calculated σ is 9.76 erg/cm^2. In view of Eq. (6), however, it is clear the σ_e value is dependent on the b_0. In other words, the difference of crystal growth surfaces may affect σ_e. Until now, most of kinetic studies on iPP crystallization proceed with the parameters of (110) lattice plane [5,24–26]. However, for those on the PP-cats, it should be more logical to calculate the σ_e by using the parameters of (040) lattice plane.

For applying the Lauritzen–Hoffman model into the crystallization kinetics of polymer blends, some modifications have been made [9–11]

$$\ln G - \ln \varphi_2 + \left[\frac{U^*}{R(T_c - T_\infty)}\right] - \frac{0.2T_m^o \ln \varphi_2}{\Delta T} = \ln G_o - \left[\frac{K_g}{T_c \cdot \Delta T \cdot f}\right] \tag{9}$$

here φ_2 is volume fraction of the crystallizable component. In present study, because the main objective is to investigate the crystallization kinetics of PP, the crystallization of ethylene–propylene block copolymer is ignored, considering a little contribution of the ethylene–propylene block copolymer to crystal phase.

The regime analysis is conducted experimentally through plotting $\ln G - \ln \varphi_2 + U^*/R(T_c - T_\infty) - 0.2T_m^o \cdot (\ln \varphi_2)/\Delta T$ vs. $1/(f \cdot T_c \cdot \Delta T)$, choosing $U^* = 6270$ J/mol, and $T_\infty = T_g - 30$ K. $T_m^o = 460$ K for iPP and $T_m^o = 455$ K for PP-cats.

According to Eq. (9), experimental data are analyzed and the results are shown in Fig. 10. The data of iPP present two lines between 117 °C and 155 °C and a transition could be observed at 138 °C, and in addition, the slope of line in high temperature range is lower than that in low temperature range. Since the value of K_g in regime II is lower than those in regimes I and III, and the temperatures corresponding to regime II are higher those of regime III, iPP curves in Fig. 10 correspond to the regimes II and III, and its abrupt change of slopes means the regime II → III transition. This result is in accord with previous reports on crystallization kinetics of iPP [5,24–26]. For iPP with high molecule weight ($M_w = 300\,000$), the regime II → III transition was observed at 137 °C [5,24–26]. Even though it was predicted that the regime I → II transition should exist at about 155 °C for iPP sample [25], no experimental proof has been achieved. However, for iPP with low molecule weight ($M_w = 15\,000$), both the regime I → II and regime II → III crystallization transitions were observed because its equilibrium melting temperature is considerably low [26].

For the PP-cats containing low content of ethylene–propylene copolymer, the similar phenomena can be found, but the transition temperature decreases with the increase of ethylene–propylene copolymer. On the other hand, for the samples containing high content of ethylene–propylene copolymer, PEP50 and PEP60, no regime II → III transition could be observed. It needs to be pointed out that for PEP60 and PEP50, the spherulite growth rate could hardly be measured when crystallization temperature is lower than 123 °C and 121 °C, respectively, because the nucleation density was too high and the impingements among spherulite quickly appeared. Since the molecular weights and polydispersity of propylene homopolymer in various PP-cats are in little difference, it suggests that these kinetic differences of PP-cats impossibly result from the molecular weights and polydispersity of propylene homopolymer.

It has been confirmed that the existence of amorphous component could affect the temperature of regime II → III transition [27]. Table 5 lists the K_g and σ_e of PP-cats and pure iPP in different regimes. It can be seen that the values of K_g and σ_e in the same regime increase with the increase of ethylene content. Since the surface nucleation barrier is positive proportion to K_g [23], the increase of K_g indicates that the increase of ethylene–propylene copolymer will lead to the decrease of surface nucleation rate. On the other hand, the increase of σ_e means the increase of the fold surface free energy of PP segment, because the increase of the fold surface free energy goes against regular folding of the molecule chain, *i.e.*, crystal growth [28]. These results are in agreement with Feng's reports [29]. Because the increase in σ_e may raise nucleation barrier and reduce nucleation rate, a larger degree of supercooling is required

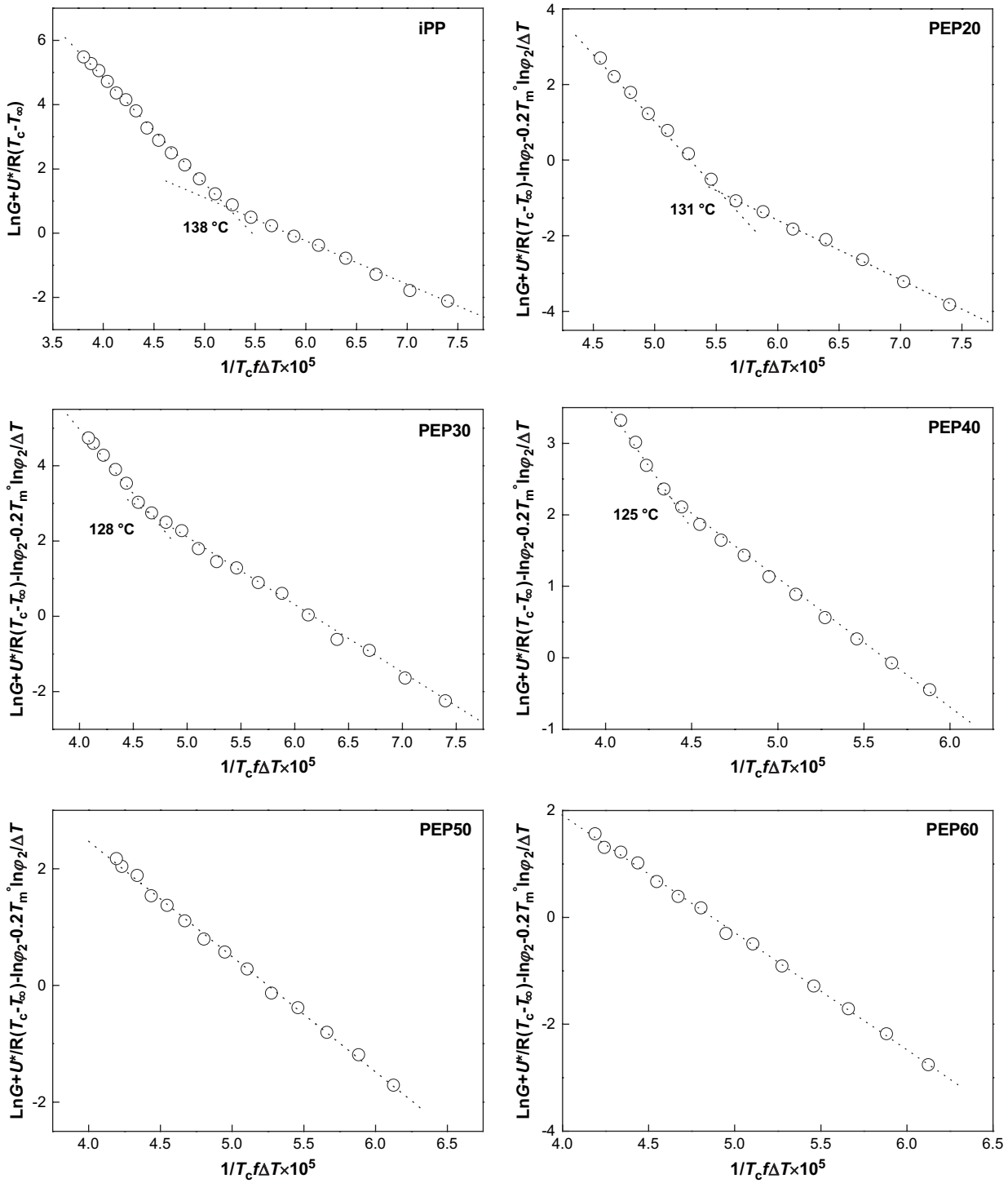

Fig. 10. Kinetic analysis of nonisothermal and isothermal growth data of iPP and PP-cats under $U^* = 6270$ J/mol and $T_\infty = T_g - 30$ K.

for the crystallization of PP-cats with higher ethylene content to enter into regime III. Furthermore, the ethylene–propylene copolymer is forced by growing PP crystal and gets together in the vicinity of crystal growth plane during crystallization. Moreover, the mobility of ethylene–propylene copolymer is very weak because of high viscosity of PP-cats, resulting in the high content of ethylene–propylene copolymer in the vicinity of crystal growth plane. These could be regard as the obstruct effect of ethylene–propylene copolymer on crystallization of PP. Beyond doubt; this obstruct effect would go simultaneity against crystal growth of PP and surface nucleation. Considering the regime II → III transition temperature shifting toward low temperature, it is reasonable to believe that the dilution effect has a stronger effect on surface nucleation than on crystal growth, and makes surface nucleation rate decrease greatly. In other words, the dilution effect of ethylene–propylene copolymer plays an important role in the shifting of the temperature of regime II → III transition.

Table 5
Various parameters determined by crystallization kinetic analysis for iPP and PP-cats

	Range (°C)	K_g(III) × 10^{-5}	σ_e (erg/cm^{-2})	Range (°C)	K_g(II) × 10^{-5}	σ_e (erg/cm^{-2})	K_g(III)/K_g(II)
iPP	117–137	3.33	81.39	139–154	1.68	82.15	1.98
PEP20	118–130	3.42	83.59	132–154	1.74	85.08	1.96
PEP30	119–127	3.56	87.01	129–154	1.83	89.48	1.94
PEP40	119–124	3.69	90.19	126–154	1.86	90.95	1.98
PEP50	–	–	–	121–154	1.97	96.33	–
PEP60	–	–	–	123–154	2.04	99.75	–

4. Conclusion

The multiple melting behavior of PP-cats is attributed to the melting of α-iPP, β-iPP and PE crystals, depending on the composition. An obvious melting point depression of PP-cats was found. Furthermore, the T_m^o value of propylene homopolymer in PP-cats seems independent of the composition and equals to 182 °C. The WAXD experimental results reveal that the existence of ethylene–propylene copolymer results in the changes of crystalline microstructure of propylene homopolymer. The kinetic analysis of PP-cats crystallization using a modified Lauritzen–Hoffman model demonstrates that there appears a regime II → III transition in iPP and PP-cats containing low content of ethylene–propylene copolymer content, *i.e.*, PEP20, PEP30 and PEP40. For the PP-cats containing high content of ethylene–propylene copolymer, *i.e.*, PEP50 and PEP60, crystallization always processes in regime II and no regime II → III transition appears. Both calculated nucleation parameter (K_g) and the fold surface free energy (σ_e) for PP-cats increase with the increase of ethylene–propylene copolymer content, indicating that the existence of ethylene–propylene copolymer goes against secondary nucleation of PP and regular folding of the molecule chain. However, taking the higher viscosity of PP-cats into account, it is believed that the increasing of viscosity results in a remarkable obstruct effect on crystallization kinetics, and this dilution effect has a stronger effect on surface nucleation as compared with crystal growth. As a result, the crystallization of PP-cats exhibits a shifting of transition temperature between regimes II and III towards low temperatures.

Acknowledgements

We are grateful for the financial supports of the National Basic Research Program of China (No. 2005CB623800), National Natural Science Foundation of China (No. 50603023) and Specialized Research Fund for the Doctoral Program of Higher Education (No. 20040335077).

References

[1] Xu JT, Feng LX, Yang SL, Wu YN, Yang YQ, Kong XM. Polymer 1997; 38:4381.
[2] Fan ZQ, Zhang YQ, Xu JT, Wang HT, Feng LX. Polymer 2001;42: 5559.
[3] Wunderlich B. Macromolecular physics. In: Crystal structure, morphology, defects, vol. 1. New York: Academic Press; 1973.
[4] Chen M, Chung CT. J Polym Sci Part B Polym Phys 1998;36: 2393.
[5] Di Lorenzo ML, Cimmino S, Silvestre C. Macromolecules 2000;33: 3828.
[6] Zheng Q, Shangguan YG, Yan SK, Song YH, Peng M, Zhang QB. Polymer 2005;46:3163.
[7] Shangguan YG, Zheng Q, Peng M. Acta Polym Sinica 2005;3:389.
[8] Shangguan YG, Zheng Q, Peng M, Wang HJ, Zhang MQ. Chem J Chinese Uni 2005;26:2386.
[9] Boon J, Aczue JM. J Polym Sci Part A-2 1968;6:885.
[10] Martuscelli E. Polym Eng Sci 1984;24:563.
[11] Alfonso GC, Russell TP. Macromolecules 1986;19:1143.
[12] Sacchi MC, Fan ZQ, Forlini F, Tritto I, Locatelli P. Macromol Chem Phy 1994;195:2806.
[13] Hoffman JD, Weeks JJ. J Res Natl Bur Stand 1962;66A:13.
[14] (a) Yamada K, Hikosaka M, Toda A, Yamazaki S, Tagashira K. Macromolecules 2003;36:4790;
(b) Yamada K, Hikosaka M, Toda A, Yamazaki S. Tagashira K. Macromolecules 2003;36:4802.
[15] Jang GS, Cho WJ, Ha CS, Kim W, Kim HK. Colloid Polym Sci. 2002; 280:424.
[16] Nitta KH, Yong-Woo SYW, Hashiguchi H, Tanimoto S, Terano M. Polymer 2005;46:965.
[17] Kakudo M, Kasai M. X-ray diffracition by polymers. Tokyo: Kodansha; 1972. p. 46.
[18] Mo ZS, Wang LX, Zhang HF, Han P, Huang BT. Acta Polym Sinica 1988;6:441.
[19] Seki M, Nakano H, Yamauchi S, Suzuki J, Matsushita Y. Macromolecules 1999;32:3227.
[20] Shangguan YG, Tao LY, Zheng Q. J Appl Polym Sci, in press.
[21] Di Lorenzo ML. Prog Polym Sci 2003;28:66.
[22] Kamal MR, Feng L. Int Polym Proc 2005;20:78.
[23] Hoffman JD, Davis GT, Lauritzen Jr JI. In: Hannay NB, editor. Treatise on solid state chemistry, vol. 3. New York: Plenum Press; 1976 [chapter 7].
[24] Clark EJ, Hoffman JD. Macromolecules 1984;17:878.
[25] Monasee B, Haudin JM. Colloid Polym Sci 1985;263:822.
[26] Cheng SZD, Janimak JJ, Zhang AQ, Cheng HN. Macromolecules 1990; 23:298.
[27] Monasee B, Haudin JM. Colloid Polym Sci 1988;266:679.
[28] (a) Hoffman JD. Polymer 1982;23:656;
(b) Hoffman JD. Polymer 1983;24:3;
(c) Hoffman JD. Polymer 1991;32:2828;
(d) Hoffman JD. Polymer 1992;33:2643;
(e) Hoffman JD, Miller RL. Polymer 1997;38:3151.
[29] Feng Y, Hay JN. Polymer 1998;26:6731.